Jenn-Yih Chen ✉
Yi-Ling Lin
Bean-Yin Lee

https://doi.org/10.21278/TOF.462033821
ISSN 1333-1124
eISSN 1849-1391

PREDICTION MODEL OF END MILL CUTTING EDGE BASED ON MATERIAL PROPERTIES AND CUTTING CONDITIONS

Summary

In machining, the cutting performance of the tool depends on the tool material, tool structure, tool geometry, properties of workpiece materials, and cutting conditions. If the user chooses an inappropriate cutting tool for the machining of the workpiece material, this will cause energy loss and severe tool wear. This study aims to investigate the influence of mechanical properties of workpiece material and cutting conditions on the tool geometry and to establish a polynomial network for the prediction of a reasonable normal relief angle and a normal wedge angle based on experimental data. Experimental results indicate that the cutting of high hardness and high strength workpiece materials requires a larger normal wedge angle to increase the cutting edge strength. In addition, the design of the normal relief angle is related to Young's modulus and the toughness of the workpiece material, mainly to avoid material elastic recovery during the cutting process. In terms of cutting parameters, as the radial depth of cut increases, the contact area between the tool and the chip increases, which causes the heat to concentrate at the tip of the tool; hence, it is necessary to increase the normal wedge angle. In addition, the feed per tooth had a negligible effect on the normal wedge angle. Finally, the prediction model was verified by five untested workpiece materials. The results of the cutting tests showed that the flatness of the cutting edge was less than 15 μm, which indicates that a normal cutting phenomenon occurred on the flank.

Key words: *cutting conditions, polynomial network, normal wedge angle, material properties*

1. Introduction

The selection of cutting tools depends on the accuracy of machining, the workpiece material, machining efficiency, and cutting form; therefore, the knowledge of selecting suitable tools for the cutting process is significant. The geometric angle of the tool has an immediate effect on the quality of the machined surface, cutting efficiency, and tool life, but how to design a reasonable geometric angle of the tool is the know-how for each tool manufacturer. To ensure the durability of the tool and fully utilize the cutting performance, it is also important to use the correct cutting parameters. Günay et al. [1] used a dynamometer to measure the variation in the main cutting force under different rake angles and cutting speeds. The experiment showed that a larger positive rake angle reduced the contact area and friction between the chip and the tool, thereby reducing the cutting forces. However, increasing the negative rake angle accelerated

the tool wear and generated a large amount of heat. Shih et al. [2] simulated the magnitude of the rake angle using finite elements which had a significant effect on the performance of the cutting tool and the integrity of the cut surface. Azaath et al. [3] studied the influence of tool geometry and shape on the contact length, cutting temperature, and tool wear rate in the simulation process of machining operations. The results presented in the study [4] suggested that the tool rake angle, relief angle, overhang of the cutting tool, feed rate, and depth of cut interact with each other and influence the machining stability simultaneously. Chen et al. [5] constructed a polynomial network with the mechanical properties of the workpiece material, provided as input to predict the tool geometry.

The radial depth of cut (a_e), axial depth of cut (a_p), feed rate (f), and cutting speed (v_c) are the cutting conditions of the end mill, which may directly affect the cutting force. As discussed in [6,7], the effect of the depth of cut and the feed rate on the cutting force is stronger than that of the cutting speed. The cutting force increases with an increase in the feed rate and the depth of cut, however; at high speeds, the cutting force decreases. The influence of the tool geometry and cutting conditions on the cutting process is demonstrated in the literature quoted above.

However, only a small number of studies have considered the workpiece material, cutting conditions, and tool geometry simultaneously when designing cutting tools. This study aims to establish a database under varying cutting conditions and mechanical properties of workpiece material, and to predict the geometrical tool angle by constructing a polynomial network model. Accordingly, it is possible to quickly predict the end mill geometry for various workpiece materials and different machining demands.

2. Cutting theory

In the metal cutting process, the geometry of the tool directly affects the cutting quality. It is necessary to define the dimensional cutting relations in advance to enhance the understanding of the mechanics of metal cutting. The cutting operation can be categorized as orthogonal or oblique; in orthogonal cutting, the cutting edge of the tool is perpendicular to the cutting direction, while in oblique cutting, it is inclined to the cutting direction, as shown in Fig. 1. The metal cutting operation belongs to the category of oblique cutting in most cases. The rake and relief angles on different planes can be divided into normal relief/rake angles and velocity relief/rake angles. The following are exhaustive definitions of angles in different directions.

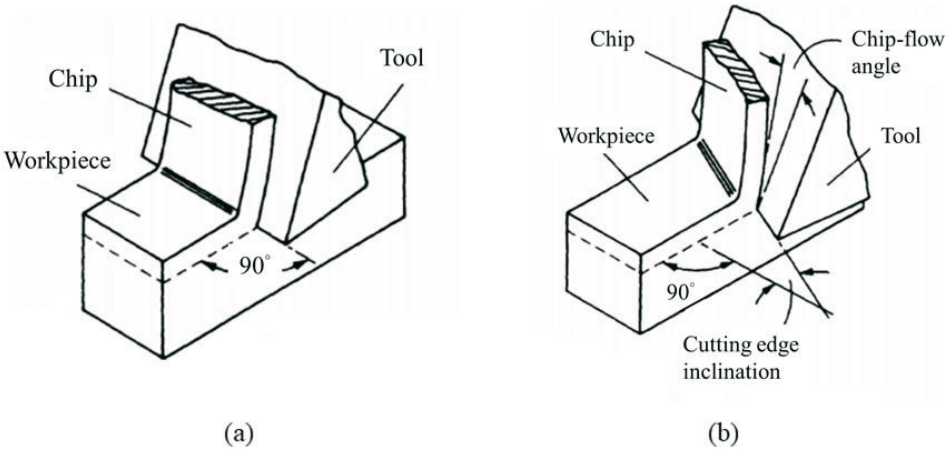

Fig. 1 (a) Orthogonal cutting (b) Oblique cutting [8]

(1) Normal rake angle (α_n): The angle between the rake face and a line perpendicular to the cutting edge, which is measured in a plane normal to the tool cutting edge.

(2) Velocity rake angle (α_v): This is the angle between the rake face and the line perpendicular to the cutting velocity vector measured in a plane parallel to the cutting velocity and normal to the machined surface.

(3) Normal relief angle (γ_n): The plane on the relief surface is perpendicular to the cutting edge. This angle and the normal rake angle together determine the wedge angle.

(4) Velocity relief angle (γ_v): The relief surface is parallel to the cutting speed direction.

The relief and rake angles in the velocity direction are set by the Walter Helitronic Tool Studio grinding software. The end mill was subjected to variations in the intermittent cutting force during the cutting process. The cutting model can be simplified into an orthogonal model to describe the state of the cutting forces. Figure 2 shows that the section of the orthogonal model is along the normal direction of the cutting edge. The rake and the relief angle in the normal direction determine the magnitude of the wedge angle. The relationship between the angles is described in Eq. (1). For workpiece materials with high hardness and strength, a larger normal wedge angle can sustain more cutting resistance and absorb the heat generated during the cutting process.

$$\alpha + \text{wedge angle} + \gamma = 90° \tag{1}$$

where α is the rake angle and γ is the relief angle.

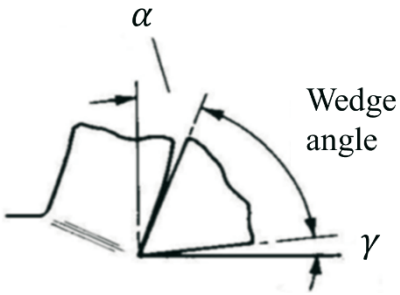

Fig. 2 A schematic drawing of orthogonal cutting

Grinding software was employed to design the tool geometry. The angle in the software is set to the velocity direction. Therefore, we must convert the angle in the normal direction into an angle in the velocity direction. Figure 3 shows the geometric relationship between the normal rake angle and the velocity rake angle. The line AD is normal to the cutting velocity vector, and the plane ABDEF is normal to the machined surface. The plane ACDGH is normal to the cutting edge, and the line CD lies in a plane normal to the cutting edge. Hence ∠EDG =∠CDB = i is the angle of obliquity.

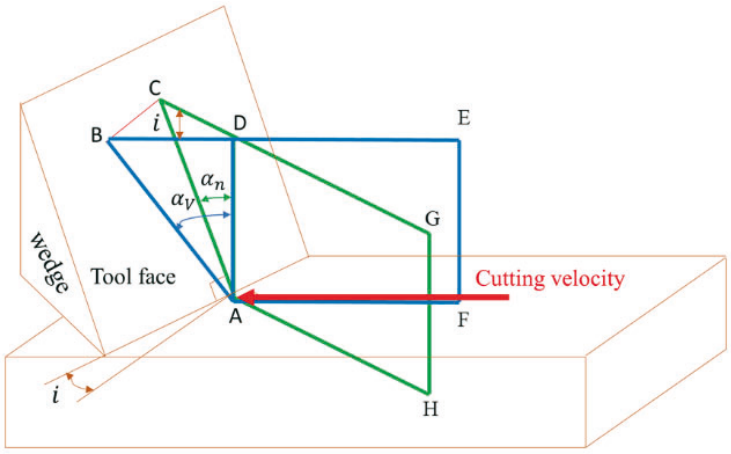

Fig. 3 Relationship between different rake angles

For the normal rake angle, we have the geometric relationship

$$\overline{CD}=\overline{AD}\times \tan \alpha_n. \tag{2}$$

For the velocity rake angle, the line BD is denoted as follows:

$$\overline{BD}=\overline{AD}\times \tan \alpha_v. \tag{3}$$

For the plane BCD, the geometric relationship is expressed as follows:

$$\overline{CD}=\overline{BD}\times \cos i. \tag{4}$$

Therefore,

$$\overline{AD}\times \tan \alpha_n =\overline{AD}\times \tan \alpha_v \times \cos i\ . \tag{5}$$

The conversion formulas between different angles are as follows:

$$\tan \alpha_v = \frac{\tan \alpha_n}{\cos i} \tag{6}$$

$$\tan \gamma_v = \tan \gamma_n \times \cos i \tag{7}$$

3. Experiment and methods

3.1 Experimental setup

The end mill cutting tool is an uncoated ultrafine round bar made of WF15 tungsten carbide, with a 30° helix angle, 6 mm diameter, and 4-flute construction. We employed the Walter Tool Studio grinding software to design the tool geometry and generate numerical control codes, which are executed by the Helitronic Basic 5-axis grinding machine used for grinding the end mill. In addition, we used the Zoller genius 3 to determine the geometry of the end mill, such as the dimensions, rake angle, relief angle, and helix angle. According to the cutting conditions suggested by the OSG catalogue for different workpiece materials, the parameters for the cutting experiment were selected by varying the radial depth of cut in the range 0.12-1.2 mm and the feed per tooth in the range 0.04-0.08 mm/tooth. We employed a Takumi B8 machine for high-speed finishing side milling under dry cutting conditions. After cutting 100 mm, an Olympus STM 6 tool microscope was used to inspect the flatness of the cutting edge to determine whether the flank was broken or chipped by material elastic recovery. This instrument can be used to measure the flank wear; the measurement position of the wear value was on the end mill radial flank. The maximum value was taken at measuring points at particular intervals on the cutting edge flank. Based on the cutting result, the normal wedge and normal relief angles of the tool were adjusted. However, it is not enough to create a prediction model that only depends on the properties of the workpiece material. Therefore, this study also investigated the effect of cutting conditions on the tool geometry. The cutting experiment had two main purposes.

1. We first observed the flank after cutting to 100 mm to check whether a rebound or a chipping phenomenon occurred. If that had happened, the normal relief angle increased. Then, after cutting to 10 m, we checked whether abnormal damage or a fracture occurred on the cutting edge of the tool; if that had happened, the normal wedge angle of the tool increased. Finally, based on the cutting experiment results, a training dataset of the normal wedge and normal relief angles of the tool was created.
2. To observe the effect of cutting conditions on the tool edge strength, only one of the desired cutting parameters was changed for each cutting test, and the rest were kept constant. The radial depth of cut used in the cutting experiments ranged from 0.12 mm to 1.2 mm, and the feed per tooth ranged from 0.04 to 0.08 mm/tooth.

3.2 Effect of mechanical properties of workpiece materials on the cutting edge strength

To examine the relationship between the mechanical properties of the workpiece material and the tool geometry, three different workpiece materials were selected for the cutting tests, as shown in Table 1. Consider SUS316L and Ti-6Al-4V workpiece materials as examples. Figures 4 and 5 show the edge condition after the workpiece materials were cut to 100 mm at different normal relief angles. When the toughness and Young's modulus of the workpiece to be machined are high, the non-uniform flank wear, chipping, and serious rebound may occur if the normal relief angle is small. Therefore, it is necessary to increase the normal relief angle.

Table 1 Mechanical properties of the tested workpiece materials

Material properties / Workpiece materials	Yield strength (MPa)	Tensile strength (MPa)	Hardness (HRC)	Shear strength (MPa)	Thermal conductivity (W/mk)	Young's modulus (GPa)	Toughness (J)
Ti-6Al-4V	880	950	36	550	6.6	113.8	17
SUS316L	290	580	17.5	530	16.3	193	105
Annealed SKD61	310	690	17.5	430	29	190	37.6

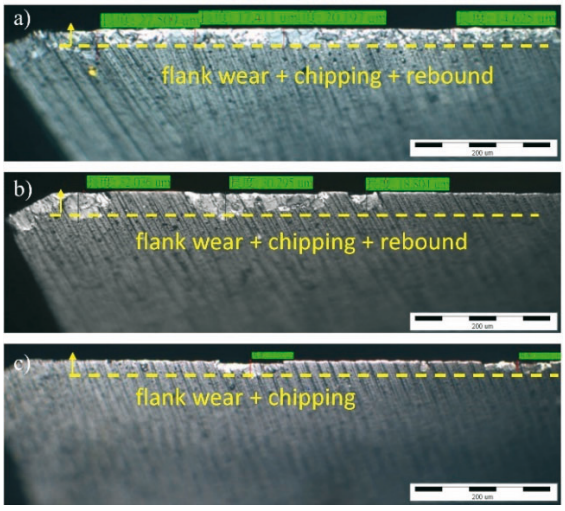

Fig. 4 Flank condition after cutting the SUS316L workpiece material to 100 mm (a) γ_n = 6.25° (b) γ_n = 11.51° (c) γ_n =14.93°

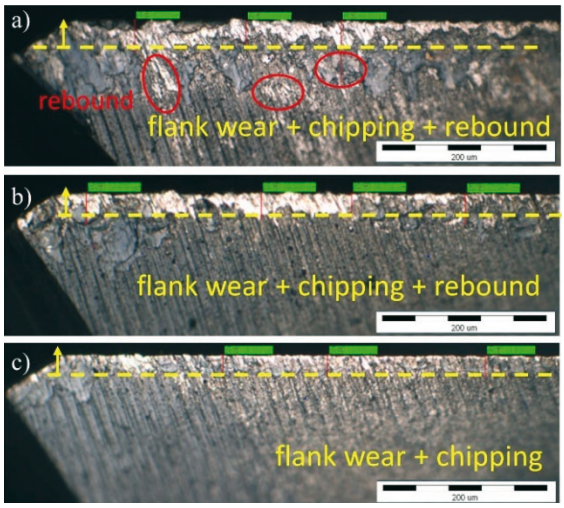

Fig. 5 Flank condition after cutting the Ti-6Al-4V workpiece material to 100 mm (a) γ_n= 2.31° (b) γ_n = 5.77° (c) γ_n =9.22°

Furthermore, we investigated the relationship between the normal wedge angle and the mechanical properties of the annealed SKD61 workpiece material by cutting; the toughness of SKD61 is between that of SUS316L and that of Ti-6Al-4V. Thus, the designed normal relief and normal wedge angles were 4.62° and 64.75°, respectively. As shown in Fig. 6, when the workpiece material is cut to 100 mm, the flatness value of the cutting edge is 2.79 μm, which indicates that the relief angle is feasible. However, when the material is cut to 10 m, the flatness value of the cutting edge is 20 μm, and a chipping phenomenon occurs on the flank, which means that the designed normal wedge angle is small, as shown in Fig. 7. Therefore, the normal wedge angle was increased by approximately 3° to improve the strength of the cutting edge. As shown in Fig. 8, it was found that there was no serious chipping on the flank of the tool, and the flank wear was approximately 6.27 μm after cutting to 10 m.

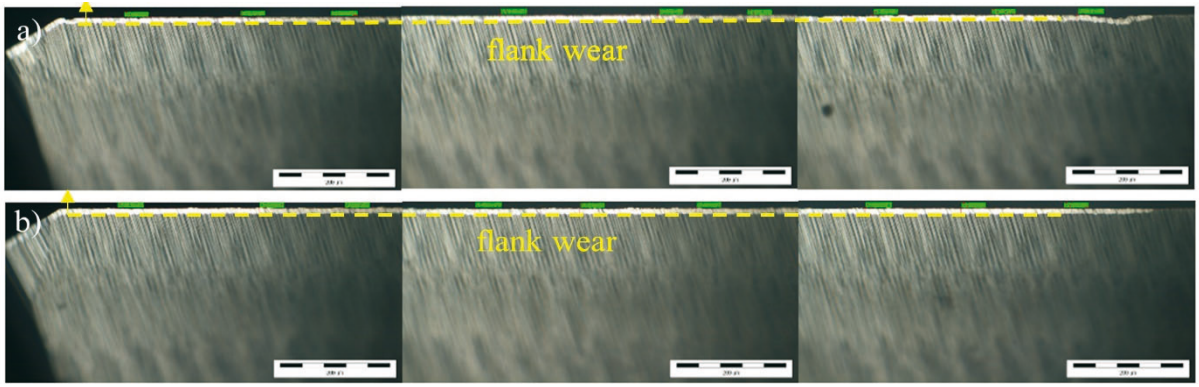

Fig. 6 Condition after cutting the annealed SKD61 to 100 mm at a normal wedge angle of 64.75° with (a) a long blade (b) a short blade

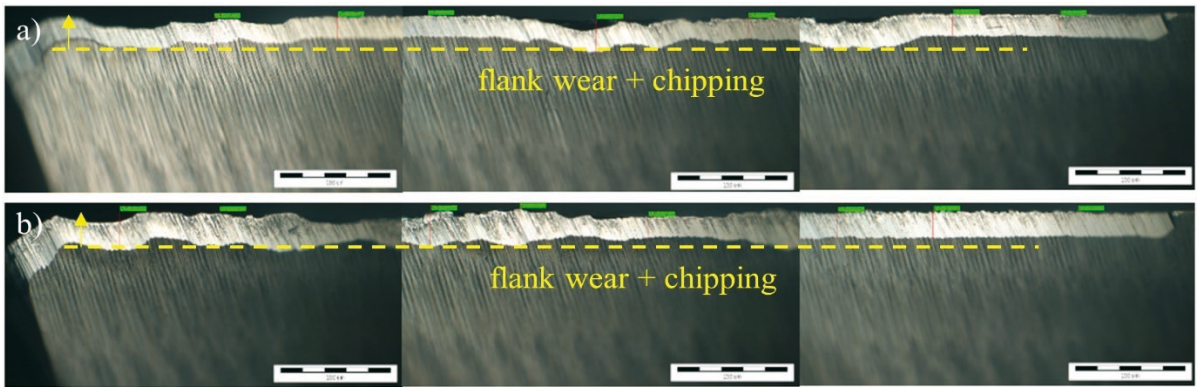

Fig. 7 Condition after cutting the annealed SKD61 to 10 m at a normal wedge angle of 64.75° with (a) a long blade (b) a short blade

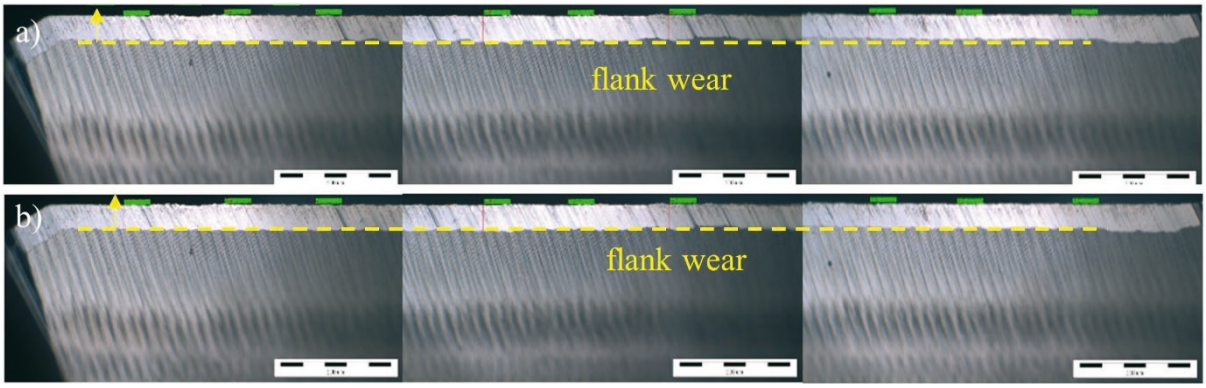

Fig. 8 Condition after cutting the annealed SKD61 to 10 m at a normal wedge angle of 68.08° with (a) a long blade (b) a short blade

The experimental results show that the normal wedge angle of the tool is based on the mechanical properties of the workpiece material such as yield strength, tensile strength, hardness, thermal conductivity, and shear strength. When a workpiece with high strength and hardness is used, the normal wedge angle of the tool is increased to prevent chipping or breakage. A workpiece with low thermal conductivity does not easily discharge the heat generated during the cutting process; thus, a large amount of heat is concentrated on the tip of the tool, which accelerates wear. Therefore, the wedge angle of the tool must also be increased to avoid rapid tool wear.

3.3 Effect of cutting conditions on the cutting edge strength

The end mill is a type of milling cutter which is widely used in the manufacturing industry. It has multiple cutting edges, which act one by one to remove chips and to generate

the requested shape of the workpiece. The cutting force on a single point of the cutting edge must be considered as it varies depending on the properties of workpiece materials, tool geometry, and cutting conditions, thereby affecting the total cutting force [9]. It is necessary to determine whether there is an overload on the tool when cutting conditions are provided. Hence, it is important to calculate the feed per tooth, which is positively correlated with the cutting efficiency, tool life, and machining accuracy.

Several cutting experiments were carried out on different workpiece materials using the geometric tools listed in Table 2. The cutting experiment was conducted by simultaneously changing the parameters one at a time while keeping the other parameters constant. The radial depth of cut ranged between 0.12 mm and 1.2 mm, the feed per tooth ranged between 0.04 mm/tooth and 0.08 mm/tooth, the axial depth of cut was fixed at 2 mm, and the cutting length was 100 mm. The process parameters are listed in Table 3.

Table 2 Tool geometric angle design

Tool geometry / Workpiece materials	Velocity rake angle (°)	Velocity relief angle (°)	Normal relief angle (°)	Normal wedge angle (°)
SUJ2	7.38	3.12	3.60	80.00
Quenched SKD61	6.34	4.00	4.62	79.89
NAK80	12.20	3.00	3.46	75.93
Ti-6Al-4V	12.20	5.00	5.77	73.63
SNCM439	13.06	6.00	6.95	71.69
Annealed SKD61	19.79	4.00	4.62	68.08
Annealed S45C	16.59	10.00	11.51	64.02
SUS304	11.60	15.00	17.19	62.73

Table 3 Cutting parameters of eight workpiece materials

Cutting condition / Workpiece materials	Spindle speed (rpm)	Feed rate (mm/min)	Radial depth of cut (mm)	Cutting speed (mm/min)	Feed per tooth(mm/tooth)
SUJ2	5300	830	0.12	100	0.04
Quenched SKD61	5300	830	0.12	100	0.04
NAK80	8000	1250	0.12	150.8	0.04
Ti-6Al-4V	5300	830	0.12	100	0.04
SNCM439	8000	1250	0.12	150	0.04
Annealed SKD61	9500	1700	0.12	179	0.04
Annealed S45C	9500	1700	0.12	179	0.04
SUS304	8000	1250	0.12	150.8	0.04

Figure 9 (a) shows the wear on the cutting tool flank after cutting the SUJ2 workpiece material to a depth of 1.2 mm at a normal wedge angle of 80°; no chipping or notch wear occurs on the cutting edge. Therefore, the normal wedge angle is decreased to 78.24°. When the radial depth of cut is increased from 0.12 mm to 0.6 mm, chipping occurs on the cutting edge as shown in Fig. 9 (b).

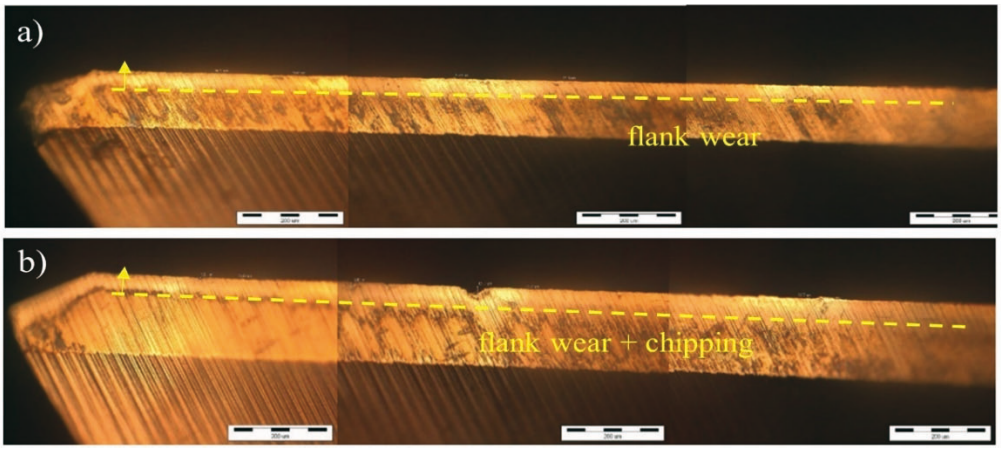

Fig. 9 Flank condition of the cutting edges after cutting the SUJ2 workpiece material (a) normal wedge angle = 80° and a_e=1.2 mm (b) normal wedge angle = 78.24° and a_e=0.6 mm

Since the experiments were conducted under dry cutting conditions, a workpiece with low thermal conductivity is more prone to a severely built-up edge owing to the difficulty in exhausting the amount of heat generated during the cutting process, as shown in Fig. 10. Therefore, the radial depth of cut was only tested up to 0.36 mm.

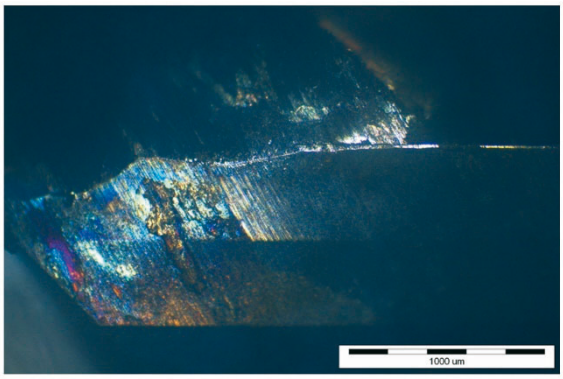

Fig. 10 Formation of built-up edges in low thermal conductivity workpiece materials

Figure 11 shows the relationship between the radial depth of cut and the normal wedge angle. When the radial depth of cut is increased, the required normal wedge angle increases correspondingly because the cutting force increases.

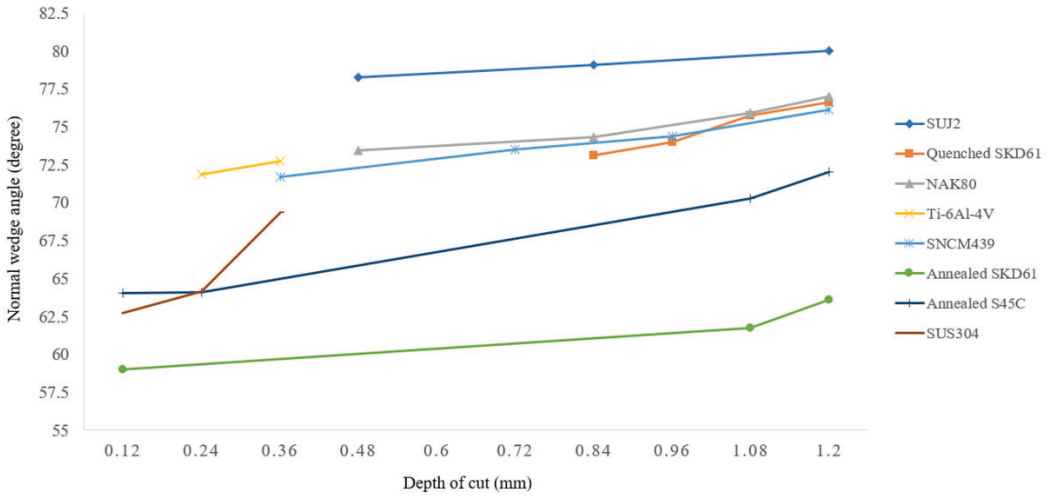

Fig. 11 Relationship between the normal wedge angle and the radial depth of cut (a_e) for different workpiece materials

Further, we examined the influence of the feed per tooth on the normal wedge angle. Figure 12 shows the condition of the flank face at a normal wedge angle of 80° after cutting the SUJ2 workpiece material to 100 mm. The flank wear is 20 μm when the feed per tooth is 0.04 mm/tooth, as shown in Fig. 12(a). When the feed per tooth is increased to 0.08 mm/tooth, the flank wear is 13 μm, as shown in Fig. 12(b), and there is no obvious chipping on the cutting edge. This indicates that the variation in this cutting parameter had little effect on the strength of the cutting edge.

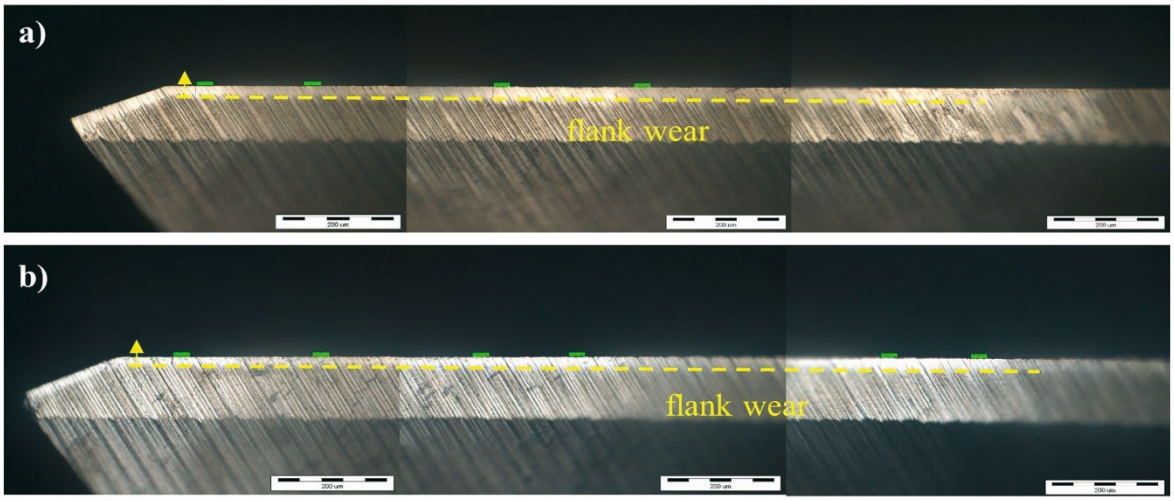

Fig. 12 Condition of the flank face (a) feed per tooth = 0.04 mm/tooth (b) feed per tooth = 0.08 mm/tooth

The test results for each workpiece material are shown in Fig. 13. Consequently, the feed per tooth can be ignored when training the model of the normal wedge angle.

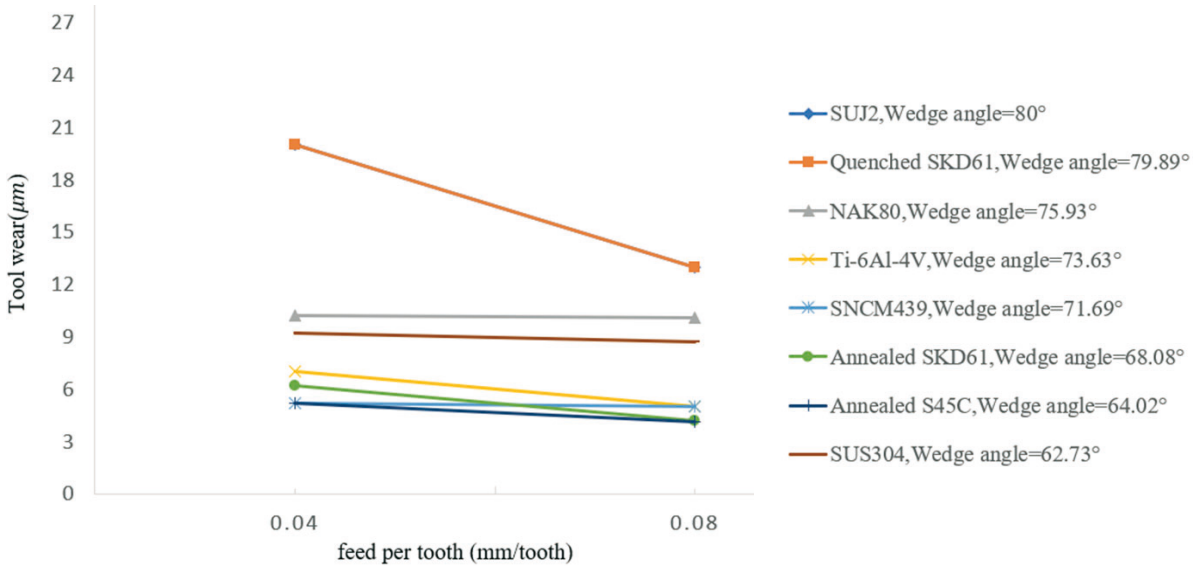

Fig. 13 Relationship between the tool wear and the feed per tooth for different workpiece materials

4. Prediction model for tool geometry

In this study, we used the polynomial network proposed by Ivakhnenho [10], which can simplify complex systems into smaller, simpler sub-systems grouped into several layers by using polynomial function nodes. The input variables of the network are transmitted into individual functional nodes. These nodes evaluate the limited number of inputs by a polynomial function and generate an output value to serve as an input to subsequence nodes of the next layer. Based on the training dataset listed in Tables 4 and 5, the abductory induction mechanism

(AIM) software was used to generate a polynomial model for predicting the normal wedge angle and the normal relief angle. The yield strength, tensile strength, hardness, shear strength, thermal conductivity, and radial depth of cut are all related to the tool edge strength, which determines the magnitude of the normal wedge angle. Young's modulus and toughness determine the normal relief angles. The predicted squared error (*PSE*) criterion [11] was used to determine the optimal network structure. The *PSE* of the training samples is composed of the two terms given in Eq. (8).

$$PSE=FSE+CPM\frac{2K}{N}S_P{}^2 \tag{8}$$

where *FSE* is the average squared error of the network in the fitting of the training data, *CPM* is the complex penalty multiplier, *K* is the number of coefficients in the network, and $S_p{}^2$ is the prior estimate of the model error variance, which is also equal to a prior estimate of *FSE*. *N* is the number of training data.

Table 4 Training data for the normal wedge angle

Workpiece materials	Properties of workpiece material					Radial depth of cut	Normal wedge angle (°)
	Yield strength (MPa)	Tensile strength (MPa)	Hardness (HRC)	Shear strength (MPa)	Thermal conductivity (W/mk)	a_e (mm)	
SUJ2	1176	1617	59	400	47	0.48	78.24
						0.84	79.11
						1.20	80.00
Quenched SKD61	1380	1590	51	890	29	0.84	73.12
						0.96	73.98
						1.08	75.73
						1.20	76.60
NAK80	1017	1264	40	760	41	0.48	73.46
						0.84	74.35
						1.08	75.93
						1.20	76.99
Ti-6Al-4V	880	950	36	550	6.6	0.24	71.87
						0.36	72.75
SNCM439	885	980	31	430	44	0.36	71.69
						0.72	73.50
						0.96	74.37
						1.20	76.11
Annealed SKD61	310	690	17.5	430	29	0.12	59.00
						1.20	63.58
Annealed S45C	343	569	13	400	51	0.12	64.02
						0.24	64.10
						1.08	70.25
						1.20	72.00
SUS304	215	505	10	545	16	0.12	62.73
						0.24	64.13
						0.36	69.34

Table 5 Training data for the normal relief angle

Workpiece materials	Properties of workpiece material		Normal relief angle (°)
	Young's modulus (GPa)	Toughness (J)	
SUJ2	190	32	3.60
Quenched SKD61	215	37.6	5.19
NAK80	207	11	3.46
Ti-6Al-4V	113.8	17	6.64
SNCM439	190	55.2	6.95
Annealed SKD61	190	37.6	4.48
Annealed S45C	200	62.4	11.20
SUS304	196	325	16.75

Figures 14 and 15 show the developed polynomial network for predicting the normal wedge angle and the normal relief angle. All polynomial equations used in the network are expressed below.

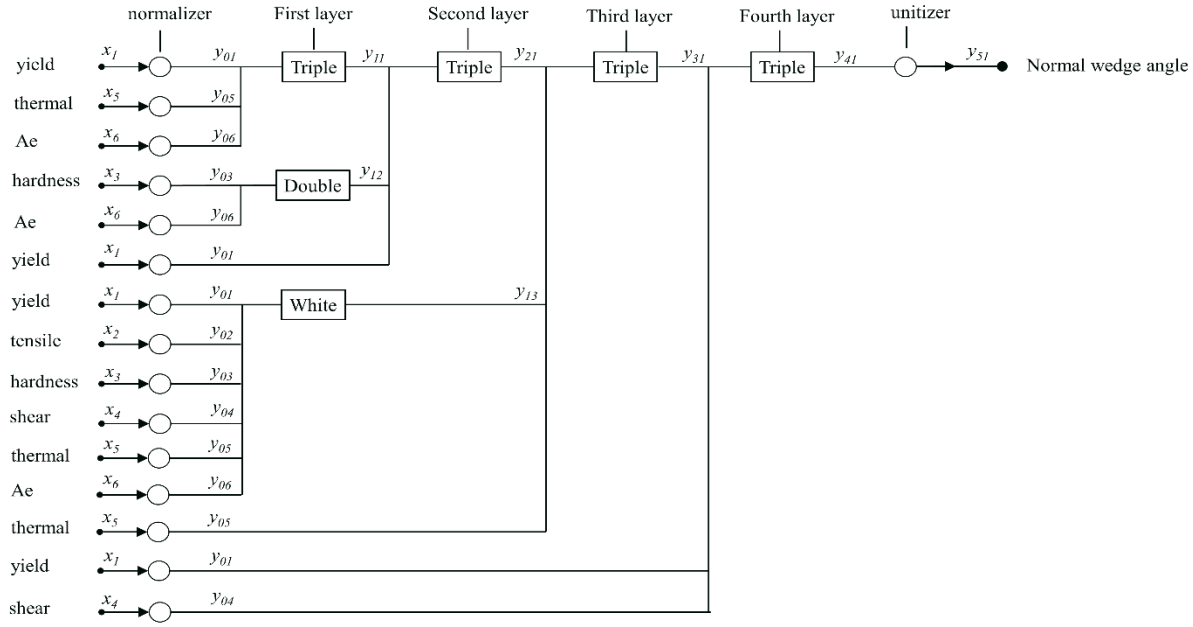

Fig. 14 A polynomial model for predicting normal wedge angle

(1) Normalizer

y_{01}=-1.76617+0.0023979x_1

y_{02}=-2.34665+0.00239786x_2

y_{03}=-1.75066+0.0586708x_3

y_{04}=-3.07569+0.00561687x_4

y_{05}=-2.52567+0.0723753x_5

y_{06}=-1.37083+2.24134x_6

(2) Triple node

$$y_{11}=-0.0631461+1.07725y_{01}-0.178581y_{05}+0.206636y_{06}-0.452167y_{01}^2+0.810217y_{05}^2 -0.214688y_{06}^2+0.311358y_{01}y_{05}+0.0867823y_{01}y_{06}-0.0579606y_{05}y_{06}-0.159962y_{01}y_{05}y_{06} -0.0463012y_{01}^3+0.338177y_{05}^3+0.223229y_{06}^3$$

$$y_{21}=-0.0853891+0.872215y_{11}+0.224787y_{12}+0.0917311y_{01}-0.387549y_{11}^2-0.683723y_{12}^2 +0.617459y_{01}^2+1.52514y_{11}y_{12}-0.663123y_{11}y_{01}-0.402613y_{12}y_{01}+0.446148y_{11}y_{12}y_{01} -0.0837887y_{11}^3-0.232225y_{12}^2-0.193808y_{01}^3$$

$$y_{31}=-0.0296848+0.966782y_{21}+0.22173y_{13}-0.0518577y_{05}+0.0554073y_{21}^2+0.0147713y_{13}^2 +0.0287318y_{05}^2-0.117375y_{21}y_{13}-0.266633y_{21}y_{05}+0.30423y_{13}y_{05}+0.104312y_{21}y_{13}y_{05} -0.0469982y_{21}^3-0.0497854y_{13}^3+0.00701901y_{05}^3$$

$$y_{41}=0.0101793+0.912762y_{31}+0.0324252y_{01}+0.0117984y_{04}+0.16373y_{31}^2+0.0629867y_{01}^2 +0.0171704y_{04}^2-0.225988y_{31}y_{01}-0.0286147y_{31}y_{04}+0.0299342y_{01}y_{04}+0.111036y_{31}y_{01}y_{04} +0.0277681y_{31}^3+0.00987047y_{01}^3-0.0416075y_{04}^3$$

(3) Double node

$$y_{12}=0.316591+0.938109y_{03}-0.293224y_{06}-0.0247633y_{03}^2-0.377481y_{06}^2-0.0628584y_{03}y_{06} -0.0992184y_{03}^3+0.523456y_{06}^3$$

(4) White node

$$y_{13}=0.298767y_{01}-3.00167y_{02}+3.19053y_{03}+0.336075y_{04}+0.289748y_{05}+0.360492y_{06}$$

(5) Unitizer

$$y_{51}=70.3624+5.64347y_{41}$$

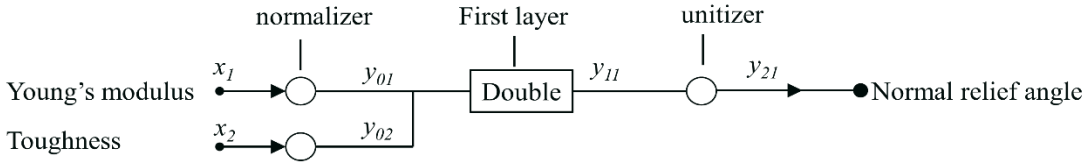

Fig. 15 A polynomial model for predicting the normal relief angle

(1) Normalizer

$$y_{01}=-6.01641+0.032049\boldsymbol{x_1}$$

$$y_{02}=-0.697315+0.00965476\boldsymbol{x_2}$$

(2) Double node

$$y_{11}=0.122499+3.59695y_{01}+2.48932y_{02}-2.13708y_{01}^2-1.32461y_{02}^2-1.65347y_{01}^3+0.205865y_{02}^3$$

(3) Unitizer

$$y_{21}=7.28375+4.56553y_{11}$$

5. Verification

To verify the accuracy of the abductive network, the mechanical properties of the five untested workpiece materials (SKS3, SUS316L, S50C, Quenched S45C, and SCM440) were fed into the polynomial network, and the normal wedge angle and the normal relief angle were calculated using the polynomial equations stated above. The predicted results are presented in

Tables 6 and 7. Using the grinding software, the rake and relief angles in the velocity direction can be obtained from Eq. (6) and (7), respectively. Further, the end geometry of the tool was designed based on Tables 6 and 7 for the cutting test. After cutting the five workpiece materials (listed above) to 100 mm, the flatness values of the cutting edge were 6.2 μm, 7.7 μm, 13.6 μm, 8.7 μm, and 10.25 μm, respectively. No obvious rebound or chipping phenomenon was observed on the flank, which indicates that a normal cutting phenomenon occurred on the flank. The conditions of the flanks after cutting the five workpiece materials to 100 mm are shown in Fig. 16. It is shown that the normal wedge and normal relief angles of the tool predicted by the AIM polynomial network model are accurate and feasible.

Table 6 Prediction results of the wedge angle obtained by the AIM polynomial network

Workpiece materials	Properties of workpiece material					Radial depth of cut	Normal wedge angle (°)
	Yield strength (MPa)	Tensile strength (MPa)	Hardness (HRC)	Shear strength (MPa)	Thermal conductivity (W/mk)	a_e (mm)	
SKS3	400	640	12	400	43	1.20	63.90
SUS316L	290	580	17.5	530	16.3	0.36	70.95
S50C	427	740	18.5	450	51	1.20	72.55
Quenched S45C	580	686	20	410	51	1.20	75.19
SCM440	835	1000	32	660	43	1.20	77.24

Table 7 Prediction results of the normal relief angle obtained by the AIM polynomial network

Workpiece materials	Properties of workpiece material		Normal relief angle (°)
	Young's modulus (GPa)	Toughness (J)	
SKS3	190	55	6.92
SUS316L	193	105	13.32
S50C	190	55.2	6.95
Quenched S45C	205	62.4	11.53
SCM440	190	47.2	5.87

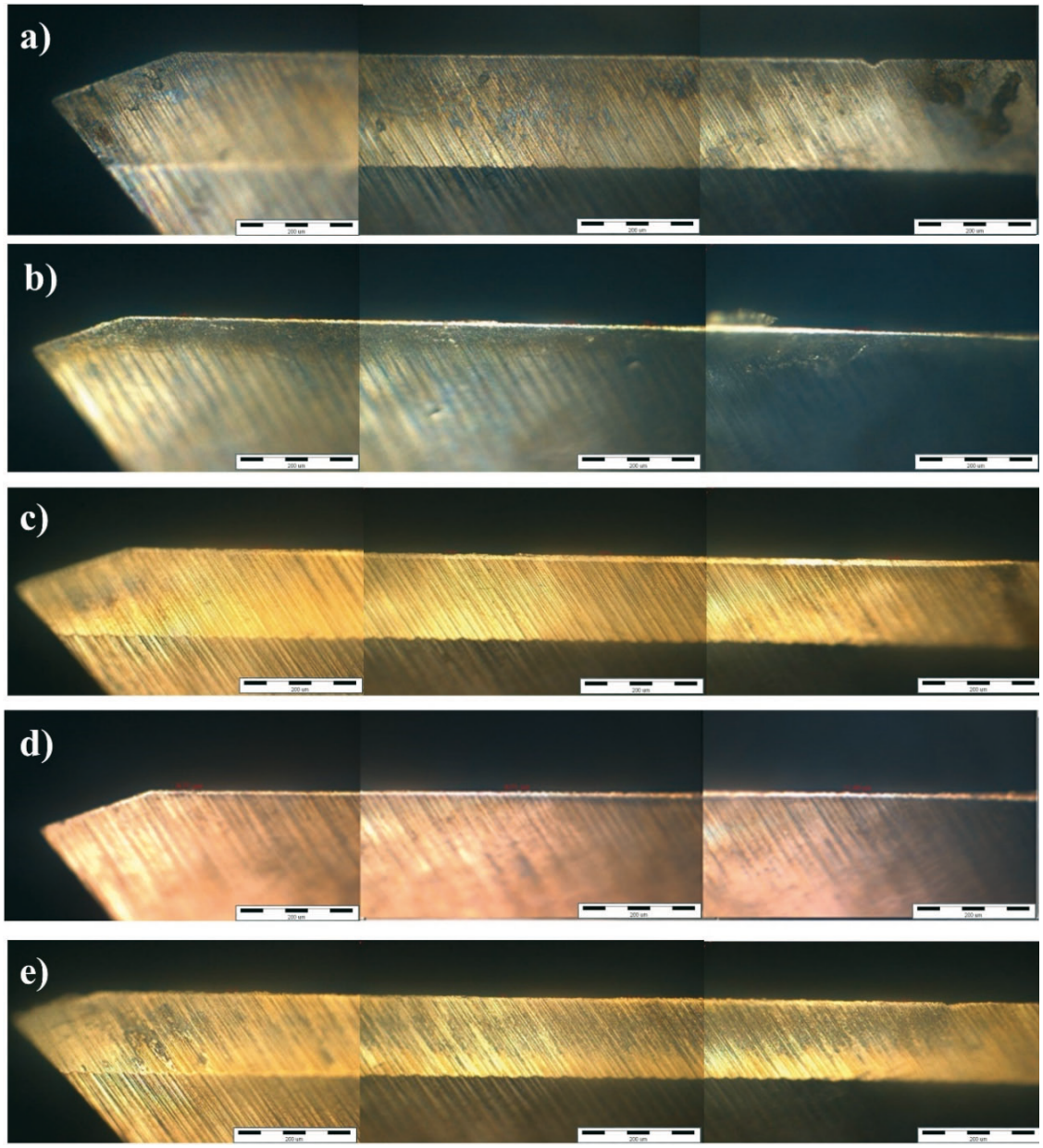

Fig. 16 Flank condition after cutting to 100 mm (a) SKS3 (b) SUS316 (c) S50C (d) Quenched S45C (e) SCM440

The marked points were the experimental data of the cutting test and the curves were obtained by the polynomial network training data. The prediction results of five verified workpiece materials show that the trends of the predicted lines and the experimental values are consistent, as shown in Fig. 17.

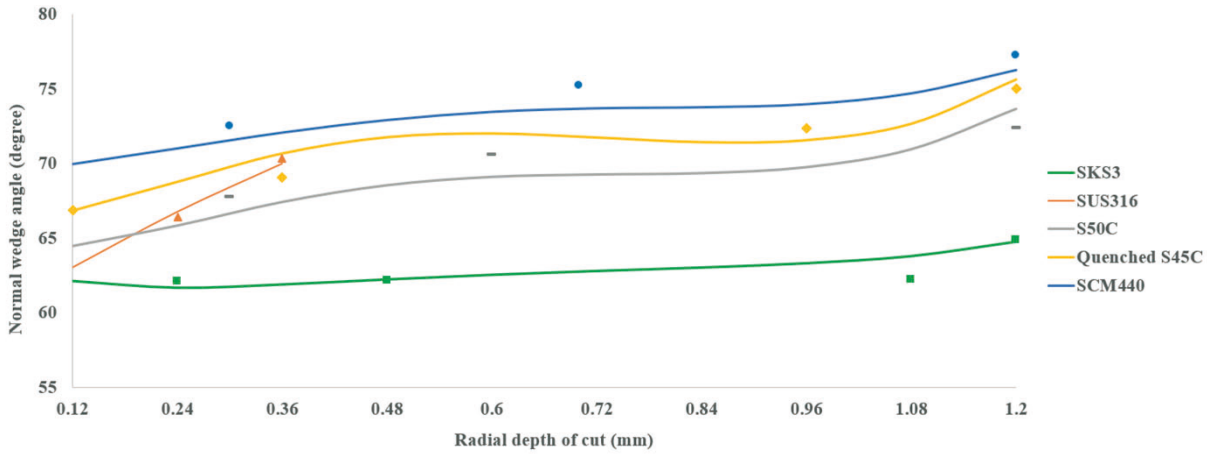

Fig. 17 Relationship between the tool normal wedge angle and the radial depth of cut (a_e) for the predicted model and experimental values

6. Conclusion

Correct and reasonable selection of process parameters and cutting tools is essential for improving the machining efficiency and product quality. The geometric design of the cutting tool directly affects the cutting performance during machining. Hence, the AIM polynomial network is used to establish the relationships among the cutting parameters, mechanical properties of workpiece materials, and geometry of the cutting tool. The predictive model can assist tool manufacturers in designing the geometric angle of the tool quickly and efficiently based on the mechanical properties of workpiece materials and cutting conditions, as opposed to a trial-and-error approach of testing and improving which wastes materials and time. The following conclusions can be drawn from previous analyses and discussions:

1. As the above experiments show, the tool wedge angle is related to the strength of the cutting edge. The direct factors affecting the strength of the cutting edge are the yield strength, tensile strength, hardness, shear strength, and thermal conductivity of the workpiece material; the design of the normal relief angle is related to Young's modulus and the toughness of the workpiece material.
2. The experimental results suggested that the normal wedge angle needs to be increased with an increase in the radial depth of cut. The variation in feed per tooth has a marginal effect on the cutting edge strength; nevertheless, the increase in feed per tooth effectively decreases the tool wear on the flank.
3. Five untested materials were put into a polynomial network model for prediction. After cutting them to 100 mm, the flatness values of the cutting edge were within 15 μm, which indicates that the verification tool did not break or get chipped.
4. The material of the tool and physical characteristics such as the stiffness of machine tool and fixture can be considered when designing the tool geometry so that the prediction model can be used in a wider range of applications.

Acknowledgment

The authors are grateful to the Ministry of Science and Technology of the R.O.C. for supporting this research (Grant Number MOST 110-2622-8-150-002) and also appreciate Yu-Sheng Lai for experimental testing and data collection.

REFERENCES

[1] M. Günay, I. Korkut, E. Aslan, U. Şeker. Experimental investigation of the effect of cutting tool rake angle on main cutting force. Journal of Materials Processing Technology. 2005, 166(1):44-49. https://doi.org/10.1016/j.jmatprotec.2004.07.092

[2] A. J. Shih. Finite element analysis of the rake angle effects in orthogonal metal cutting. International Journal of Mechanical Sciences. 1995, 38(1):1-17. https://doi.org/10.1016/0020-7403(95)00036-W

[3] L. M. Azaath, E. Mohan, U. Natarajan. Effect of rake angle and tool geometry during machining process of AISI 4340 steel in finite element approach. Materials Today: Proceedings, 2021, 37(3):3731-3736. https://doi.org/10.1016/j.matpr.2020.10.196

[4] S. Saravanamurugan, B. S. Sundar, R. S. Pranav, A. Shanmugasundaram. Optimization of cutting tool geometry and machining parameters in turning process. Materials Today: Proceedings. 2021, 38(3-5): 3351-3357. https://doi.org/10.1016/j.matpr.2020.10.246

[5] J. Y. Chen, T. C. Chan, B. Y. Lee, C.Y. Liang. Prediction model of cutting edge for end mills based on mechanical material properties. International Journal of Advanced Manufacturing Technology. 2020, 107:2939-2951. https://doi.org/10.1007/s00170-019-04884-8

[6] V. Sivaraman, S. Sankaran, L. Vijayaraghavan. The effect of cutting parameters on cutting force during turning multiphase microalloyed steel. Procedia CIRP. 2012, 4:157-160. https://doi.org/10.1016/j.procir.2012.10.028

[7] B. Tulasiramarao, K. Srinivas, P. R. Reddy, A. Raveendra, B. V. R. Ravi Kumar. Finding cutting forces while turning operation on lathe machine at different depth of cut of different metals. International Journal of Innovative Research in Science. 2014, 3(10):16866-16872. https://doi.org/10.15680/IJIRSET.2014.0310065

[8] B. L. Juneja. 2003. Fundamentals of Metal Cutting and Machine Tools. Halsted Press, New Age International.

[9] M. Bourdim, A. Bourdim, S. Kerrouz. Influence of cutting parameters on cutting forces. International Journal of Materials, 2017, 4:26-30.

[10] A. G. Ivakhnenko. Polynomial theory of complex systems. IEEE Transactions on Systems, Man, and Cybernetics, 1971, 1(4):364 -378, https://doi.org/10.1109/TSMC.1971.4308320

[11] A. R. Barron. 1984. Predicted squared error: a criterion for automatic model selection. S. J. Farlow, Self-Organizing Methods in Modeling: GMDH Type Algorithms. CRC Press, Marcel Dekker, New York, pp. 87-104.

Submitted: 21.8.2021

Accepted: 07.3.2022

Jenn-Yih Chen*
Department of Mechanical and Computer-Aided Engineering, National Formosa University, Yunlin 632, Taiwan, R.O.C.
Yi-Ling Lin
Department of Power Mechanical Engineering, National Formosa University, Yunlin 632, Taiwan, R.O.C.
Bean-Yin Lee
Department of Mechanical and Computer-Aided Engineering, National Formosa University, Yunlin 632, Taiwan, R.O.C.
*Corresponding author:
jychen@nfu.edu.tw